DOI: 10.61782/fa.2023.0909

forum acusticum 2023

IMPLEMENTATION AND APPLICATION OF THE CONVECTED BEM FOR THE SIMULATION OF MOVING SOURCES

Péter Fiala[1*] **Péter Rucz**[1]

[1] Department of Networked Systems and Services, Faculty of Electrical Engineering and Informatics, Budapest University of Technology and Economics, Műegyetem rkp. 3., H-1111 Budapest, Hungary.

ABSTRACT

The simulation of spatially extended moving sound sources plays an important role in several applications, such as virtual acoustics, tracking of moving sources, or the simulation of traffic induced noise. The main computational challenges are the proper representation of the source trajectory, the reproduction of the Doppler effect, and the incorporation of the frequency dependent source directivity. For spatially extended sources, the boundary element method is a feasible choice for computing the radiated field in the frequency domain. However, the application of the BEM restricts the source trajectory to uniform motion, where the radiation problem is equivalent to that of a stationary source in uniform flow. In this paper we present the implementation of the convected BEM in the open source C++ framework NiHu. The paper discusses the computational challenges including the problem of fictitious eigenfrequencies and frequency-to-time domain transforms. Besides presenting the validation test cases, the application of the methodology in a simulation environment for beamforming methods is addressed.

Keywords: *convected BEM, directivity, moving sound sources*

**Corresponding author*: *fiala@hit.bme.hu.*

1. INTRODUCTION

The realistic simulation of the sound field emitted by moving sources plays an important role in the fields of virtual acoustics and environmental noise. While the simulation of monopole sources moving along arbitrary trajectories is straightforward, the reproduction of the field of a spatially extended, i.e. directed, moving source is challenging, as the interaction of wave fields radiated from distinct parts of the radiator needs to be tackled. This interaction problem can be formulated as a boundary value problem in a moving medium [1, 2], and leads to the convected wave equation or Galbrun's equation for non-uniform flows. Finite element solutions of the convected wave equation [3] or Galbrun's equation [4] were presented recently, but these techniques cannot be applied for radiation into the infinite space. The present paper addresses the solution of the convected wave equation in uniform flows and in infinite domains, using the BEM.

2. SIMULATION OF MOVING POINT SOURCES IN TIME DOMAIN

2.1 Time domain simulation

The sound field radiated by a moving acoustic source is generally described by the integral

$$p(\mathbf{x},t) = \int_{\boldsymbol{x}_s}\int_{t_s} q(\boldsymbol{x}_s,t_s)h(\boldsymbol{x},\boldsymbol{x}_s,t,t_s)\,\mathrm{d}t_s\,\mathrm{d}\boldsymbol{x}_s, \quad (1)$$

where $p(\boldsymbol{x},t)$ denotes the sound pressure at location $\boldsymbol{x}$ and time t, $q(\boldsymbol{x}_s,t_s)$ is the source strength at the source location $\boldsymbol{x}_s$ and source time t_s, and h denotes the time variant transfer function, depending on the source and the acoustic medium. For the simple case of a monopole source,

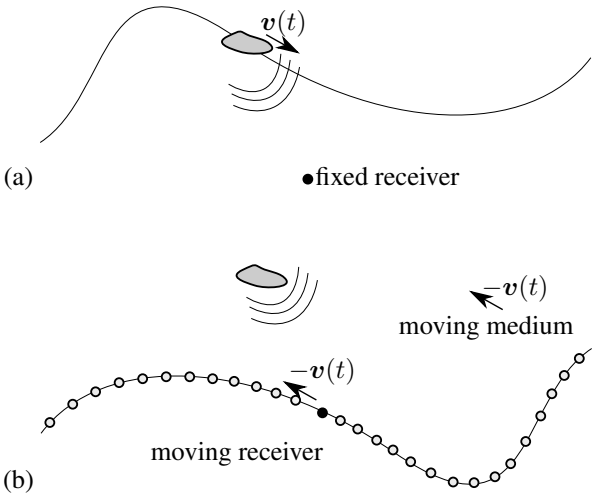

Figure 1. Simulation of the field of a moving source in (a) a frame of reference fixed to the receiver, or (b) in a frame of reference fixed to the source

the transfer function is expressed as

$$h(\boldsymbol{x}, \boldsymbol{x}_s(t_s), t, t_s) = \frac{\delta(\boldsymbol{x} - \boldsymbol{x}_s)\delta\left(t - t_s - \frac{|\boldsymbol{x}-\boldsymbol{x}_s(t_s)|}{c}\right)}{4\pi|\boldsymbol{x} - \boldsymbol{x}_s(t_s)|}, \tag{2}$$

with δ being the Dirac delta and c denoting the speed of sound. This allows for computing the field of moving monopole sources directly in the time domain. However, for spatially extended, directive sources, the time variant transfer function h is generally unknown, and its numerical computation is a challenging task, even for the simplest case of uniform motion.

As an alternative, the radiated sound field can be computed in a moving frame of reference fixed to the moving source [as shown in Figure 1(b)]. For the case of uniform motion and free field radiation in a homogeneous medium, the source-to-receiver transfer function becomes time invariant in the moving frame of reference, which simplifies the convolution (1) to the form

$$p(\boldsymbol{x}', t) = \int_{\boldsymbol{x}'_s} \int_{t_s} q(t_s) h'(\boldsymbol{x}' - \boldsymbol{x}'_s, t - t_s)\, \mathrm{d}t_s\, \mathrm{d}\boldsymbol{x}'_s, \tag{3}$$

where $\boldsymbol{x}'_s$ is the stationary source position, and h' denotes the transfer function in a medium that flows with the uniform velocity $-\boldsymbol{v}$.

2.2 Convolution quadratures

Convolution quadratures [5] is a means to temporally approximate convolution integrals of the form

$$y(t) = \int_0^t h(t - t_s) g(t_s)\, \mathrm{d}t_s, \qquad 0 \le t \le T \tag{4}$$

when the temporal representation of the transfer h is singular or even not available, as long as its complex frequency domain counterpart can be computed. The temporal convolution is approximated using the discrete form

$$y_k = \sum_{m=0}^{k} \omega_{k-m}(\hat{h}, \Delta t) g_m, \qquad k = 0, \ldots, N, \tag{5}$$

where $y_k = y(k\Delta t)$ and $g_k = g(k\Delta t)$ denote equidistant samples of the response and the excitation, Δt is the time step, and $\omega_k(\hat{h}, \Delta t)$ denotes the k-th quadrature weight, dependent on the Laplace transformed convolution kernel $\hat{h}$ and the time step. For the case of multistep convolution quadratures [5,6], the quadrature weights are computed as

$$\omega_k(\hat{h}, \Delta t) = \frac{1}{2\pi \mathrm{i}} \int_{|z|=\mathcal{R}} \hat{h}\left(\frac{\gamma(z)}{\Delta t}\right) z^{-k-1}, \tag{6}$$

where $\hat{h}(s)$ denotes the kernel in the complex frequency domain, $\gamma(z)$ is the quotient of the generating polynomial of a linear multistep method, and the integration radius $\mathcal{R}$ is chosen to be within the domain of analyticity of the kernel $\hat{h}$. The integral in (6) can be approximated by a trapezoidal rule in polar coordinates, yielding

$$\omega_k(\hat{h}, \Delta t) \approx \frac{\mathcal{R}^{-k}}{L} \sum_{l=0}^{L-1} \hat{h}\left(s_l\right) \mathrm{e}^{-\mathrm{i}kl2\pi/L}, \tag{7}$$

where $s_l = \gamma\left(\mathcal{R}\mathrm{e}^{\mathrm{i}l2\pi/L}\right)/\Delta t$ denotes the complex frequency samples.

Recently, Banjai [7] suggested to define the convolution weights ω_k for negative k indices using the same formula (7), practically resulting in $\omega_{-1} = \omega_{-2} \cdots = 0$. Utilising this redefinition, the upper summation limit k in (5) can be extended to $L - 1$ (assuming $L \ge N$), and the following relation is obtained between samples of the excitation g_m and the response y_k:

$$\mathcal{R}^k y_k = \frac{1}{L} \sum_{l=0}^{L-1} \hat{h}\left(s_l\right) \mathrm{e}^{-\mathrm{i}kl2\pi/L} \sum_{m=0}^{L-1} \mathcal{R}^m g_m \mathrm{e}^{\mathrm{i}ml2\pi/L}. \tag{8}$$

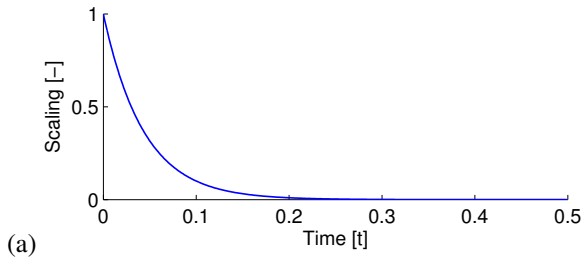

(a)

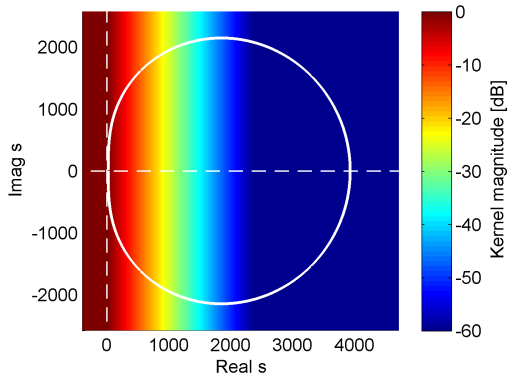

(b)

Figure 2. (a) Scaling function $\mathcal{R}^k$ (9) used for pre-attenuation in the time domain. (b) The kernel is evaluated in the s-domain along a closed trajectory.

Equation (8) defines an efficient transformation method to evaluate the linear convolution in the complex frequency domain. The s-domain representation $\hat{x}(s_l)$ of a discrete time domain function x_k is defined by the transformation pair

$$\hat{x}(s_l) = \sum_{k=0}^{L-1} \mathcal{R}^k x_k \mathrm{e}^{\mathrm{i}kl2\pi/L}, \tag{9}$$

$$\mathcal{R}^k x_k = \frac{1}{L} \sum_{l=0}^{L-1} \hat{x}(s_l) \mathrm{e}^{-\mathrm{i}kl2\pi/L}, \tag{10}$$

and (8) is equivalently expressed by the multiplication $\hat{y}(s_l) = \hat{h}(s_l)\hat{g}(s_l)$.

Convolution quadratures decouple the acoustic radiation problem (3) in a moving medium into independent Helmholtz problems. The source time history is transformed into the frequency domain by pre-attenuating by the exponential function shown in Figure 2(a) and performing a Discrete Fourier Transform (9). The response in the complex frequency domain is obtained by multiplication with the kernel, evaluated along a closed trajectory in the complex frequency domain, as shown in Figure 2(b). Finally, the response is obtained by an inverse DFT and compensation of the pre-attenuation (10).

3. BEM MODELLING IN THE COMPLEX FREQUENCY DOMAIN

3.1 Problem statement

This section describes the numerical computation of the harmonic sound field radiated by a vibrating source in a moving medium. The medium is characterized by its mass density ρ, speed of sound c, and the Mach number vector $\boldsymbol{M} = \boldsymbol{v}/c$ of the uniform flow, where $\boldsymbol{v}$ is the flow velocity. Only subsonic flow velocities are considered, meaning that $M = |\boldsymbol{M}| < 1$. The PDE to be solved is formulated in the frequency domain in the form of the convected Helmholtz equation [1]:

$$\nabla_y^2 p(\boldsymbol{y}) - M^2 p''_{mm}(\boldsymbol{y}) - 2\mathrm{i}kMp'_m(\boldsymbol{y}) + k^2 p(\boldsymbol{y}) = 0, \tag{11}$$

where $p(\boldsymbol{y})$ is the frequency content of the sound pressure in point $\boldsymbol{y}$, $k = \omega/c$ is the scalar acoustic wave number, and $p'_m(\boldsymbol{y}) = \nabla_y p(\boldsymbol{y}) \cdot \boldsymbol{e}_M$ denotes the derivative of the pressure in the flow direction $\boldsymbol{e}_M = \boldsymbol{M}/M$. The PDE's boundary condition (BC) is prescribed normal acoustic particle velocity $v_n(\boldsymbol{y}) = -p'_n(\boldsymbol{y})/(\mathrm{i}\omega\rho)$ along the boundary of the closed radiator.

3.2 Boundary integral equations

In order to formulate the boundary integral equations, the fundamental solution $G(\boldsymbol{x}, \boldsymbol{y})$ of the adjoint operator of the convected Helmholtz equation is introduced [1,2]. The fundamental solution is defined by the equation

$$\nabla_y^2 G(\boldsymbol{x}, \boldsymbol{y}) - M^2 G''_{m_y m_y}(\boldsymbol{x}, \boldsymbol{y}) + 2\mathrm{i}kMG'_{m_y}(\boldsymbol{x}, \boldsymbol{y}) + k^2 G(\boldsymbol{x}, \boldsymbol{y}) = -\delta(\boldsymbol{y} - \boldsymbol{x}), \tag{12}$$

and it describes the pressure field in $\boldsymbol{y}$ induced by a monopole source located at $\boldsymbol{x}$, when the transmitting medium moves with the opposite flow velocity $-\boldsymbol{v}$ (note the sign of the 3rd term). Testing the PDE with the fundamental solution, integrating by parts twice and applying the Gauss theorem with a normal vector pointing towards the acoustic field, the following integral representation is

obtained:

$$c(\boldsymbol{x})p(\boldsymbol{x}) = \int_S \mathcal{L}_y\{G(\boldsymbol{x},\boldsymbol{y})\}\, p(\boldsymbol{y}) - G(\boldsymbol{x},\boldsymbol{y})\mathcal{L}_y\{p(\boldsymbol{y})\} + 2\mathrm{i}kMG(\boldsymbol{x},\boldsymbol{y})p(\boldsymbol{y})n_m(\boldsymbol{y})\,\mathrm{d}\boldsymbol{y}, \quad (13)$$

where the newly introduced operator $\mathcal{L}_y\{\cdot\}$ is defined as

$$\mathcal{L}_y\{\phi\} = \phi'_{n_y} - M^2\phi'_{m_y}n_m, \quad (14)$$

and $n_m(\boldsymbol{y}) = \mathbf{n}(\boldsymbol{y})\cdot\mathbf{e}_M$ is the flow direction component of the normal vector. The term $c(\boldsymbol{x})$ on the left-hand side is given as

$$c(\boldsymbol{x}) = \begin{cases} 1 & \text{in the acoustic domain,} \\ 1/2 & \text{on a smooth boundary,} \\ 0 & \text{inside the radiator.} \end{cases} \quad (15)$$

3.3 Separating tangential and normal derivatives

The boundary integral equation (13) involves the directional derivative of the surface pressure p'_m in the direction of the Mach vector. This directional derivative must be decomposed into normal and tangential components. The unit Mach number vector is decomposed into normal and tangential components as

$$\boldsymbol{e}_m = (\boldsymbol{e}_m\cdot\boldsymbol{n})\,\boldsymbol{n} + (\boldsymbol{e}_m\cdot\boldsymbol{t})\,\boldsymbol{t} = n_m\boldsymbol{n} + t_m\boldsymbol{t}, \quad (16)$$

where $\boldsymbol{n}$ is the surface unit normal, and $\boldsymbol{t}$ is the surface unit tangential defined by the projection of the Mach number vector onto the surface. Using the decomposition, the Mach directional derivative can be expressed as $p'_m = p'_n n_m + p'_t t_m$, and the operator $\mathcal{L}_y\{p\}$ can be expressed as

$$\mathcal{L}_y\{p\} = p'_{n_y}\left(1 - M^2n_m^2\right) - M^2p'_{t_m}n_m, \quad (17)$$

where the notation p'_{t_m} has been introduced as the tangential Mach vector directional derivative.

With separating the normal and tangential components, the CBIE (13) is written as

$$c(\boldsymbol{x})p(\boldsymbol{x}) = \int_S \left[G'_{n_y} + 2\mathrm{i}kMGn_m - M^2G'_{m_y}n_m\right] p\,\mathrm{d}\boldsymbol{y} - \int_S G\left[1 - M^2n_m^2\right]p'_{n_y}\,\mathrm{d}\boldsymbol{y} - \int_S GM^2n_m\,p'_{t_m}\,\mathrm{d}\boldsymbol{y}. \quad (18)$$

In (18) the three integrals contain (i) the pressure, (ii) its normal derivative, and (iii) its Mach number directional tangential derivative, respectively.

3.4 Discretization and solution

In order to solve the integral equation, the surface pressure and its derivatives are discretized by introducing the shape functions $N_j(\boldsymbol{y})$.

$$p(\boldsymbol{y}) = \sum_j N_j(\boldsymbol{y})p_j \quad (19)$$

$$p'_{n_y}(\boldsymbol{y}) = \sum_j N_j(\boldsymbol{y})p'_{nj} \quad (20)$$

$$p'_{t_m}(\boldsymbol{y}) = \sum_j N'_{j\,t_m}(\boldsymbol{y})p_j \quad (21)$$

Note that the tangential derivatives are approximated using the pressure nodal values p_j and the tangential derivatives of the interpolation functions. Evaluating the boundary integrals in collocation points $\boldsymbol{x}_i$, the following system of linear equations is obtained: $\mathbf{Cp} = \mathbf{Hp} - \mathbf{Gq}$, where $\mathbf{C} = \mathrm{diag}\,\{c(\boldsymbol{x}_i)\}$,

$$G_{ij} = \int_S G(\boldsymbol{x}_i,\boldsymbol{y})\left[1 - M^2n_m^2\right]N_j(\boldsymbol{y})\,\mathrm{d}\boldsymbol{y}, \quad (22)$$

and

$$H_{ij} = \int_S \left[G'_{n_y}(\boldsymbol{x}_i,\boldsymbol{y}) + 2\mathrm{i}kMG(\boldsymbol{x}_i,\boldsymbol{y})n_m - M^2G'_{m_y}(\boldsymbol{x}_i,\boldsymbol{y})n_m\right]N_j(\boldsymbol{x})\,\mathrm{d}\boldsymbol{y} - \int_S G(\boldsymbol{x}_i,\boldsymbol{y})M^2n_m\,N'_{j\,t_m}(\boldsymbol{y})\,\mathrm{d}\boldsymbol{y}. \quad (23)$$

4. CONVECTED BEM IMPLEMENTATION

The BEM described in Section 3 has been incorporated into the generic BEM template library NiHu. NiHu [8] is a C++ template library with the primary purpose to efficiently evaluate discretized weighted residual integrals of the form

$$K_{ij} = \int_S T_i(\boldsymbol{x}) \int_S \mathcal{K}(\boldsymbol{x},\boldsymbol{y})N_j(\boldsymbol{y})\,\mathrm{d}S, \quad (24)$$

where $\mathcal{K}$ is a kernel function, $N_j(\boldsymbol{y})$ is a trial function space defined over a discretized mesh of the boundary surface S, and T_i is a test function space. The generic template library provides the automatic selection of efficient integration algorithms for specific families of regular or singular kernel functions and various predefined function spaces in two and three dimensions. Incorporating a new

BEM formulation into the framework involves the definition of the new kernel function alongside with its properties, such as symmetry and asymptotic behavior. This allows the framework to select proper numerical integration methods for the efficient evaluation of the weighted residual. Predefined constant, isoparametric, and Gaussian function spaces can be selected as interpolation (trial) functions. Collocational formulations are implemented by selecting Dirac delta function spaces as test function space: $T_i(\boldsymbol{x}) = \delta(\boldsymbol{x}_i)$. For Galerkin formulations, the test and trial function spaces are identical: $T_i = N_i$.

The incorporation of the convected BEM necessitated the extension of the NiHu library by a new family of directional derivative function space $\mathcal{D}_M(N_j)$. This directional derivative function space, when evaluated in a surface location $\boldsymbol{y}$, evaluates the tangential directional derivative of the interpolation function in the direction $\boldsymbol{M}$.

5. FICTITIOUS EIGENFREQUENCIES

It is well known that the BEM solution of the Helmholtz equation is prone to the fictitious eigenfrequency problem. When solving an exterior Neumann problem, the BEM fails to yield a unique solution at the eigenfrequecies of the corresponding interior Dirichlet problem. Several mitigation methods have been proposed in order to avoid the fictitious eigenfrequency problem. The two most widely used methods are the CHIEF (Combined Integral Equation Formalism) [9] and the Burton – Miller approaches [10]. The CHIEF method exploits the fact that the spurious solutions can be excluded by extending the system of equations by additional internal collocation points. The internal collocation points must not be placed on the nodal positions of the spurious modes, therefore, in practice, a sufficiently large number of random internal CHIEF points are applied. The resulting overdetermined system of equations takes the form

$$\begin{pmatrix} \frac{1}{2}\mathbf{p} \\ \mathbf{0} \end{pmatrix} = \begin{bmatrix} \mathbf{H} \\ \mathbf{H}_c \end{bmatrix} \mathbf{p} - \begin{bmatrix} \mathbf{G} \\ \mathbf{G}_c \end{bmatrix} \mathbf{q}. \tag{25}$$

The Burton – Miller approach couples the original integral equation with its normal derivative. Its drawback is that its application results in the evaluation of strongly and hypersingular integrals in the Cauchy Principal Value (CPV) and Hadamard Finite Part (HFP) sense.

The following numerical simulation shows the mitigation of fictitious eigenfrequencies by means of the CHIEF method. The modelled problem is a "transparent sphere" case, where an acoustic monopole is placed inside a sphere, and its pressure and velocity fields are evaluated on the boundary of the sphere. The velocity field is then imposed as a Neumann BC of an external radiation problem, and the pressure solution on the surface is compared to the analytical pressure field of the monopole.

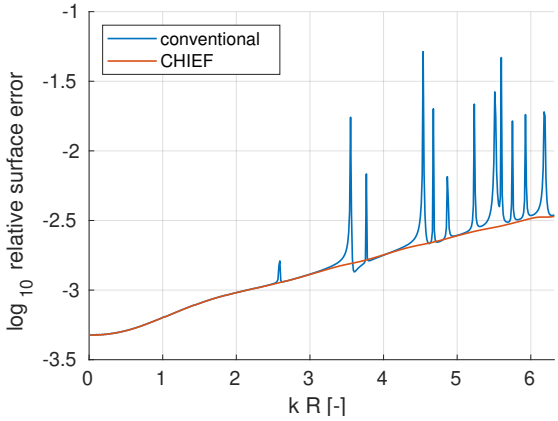

Figure 3. Relative error of an external Neumann problem solved by the conventional BEM and the CHIEF, for the case of a vibrating sphere model.

The modelled unit sphere is discretized by 1536 quadrilateral surface elements. The pressure and velocity fields are approximated using 4 Gaussian interpolation points per element, resulting in 6144 pressure unknowns. The 384 CHIEF points are uniformly distributed along the surface of a cube of unit side length, centered at the origin.

The resulting overdetermined 6528×6144 system of linear equations is solved in the LS-sense by explicit premultiplication by the transpose of the system matrix, followed by the application of a GMRES iterative solver [11]. It is worth noticing that premultiplication with the dense system matrix is computationally more demanding than carrying out the 50 to 80 GMRES iterations to reach a backward error of 10^{-10}.

Figure 3 displays the relative error of the surface pressure with and without the CHIEF method, in the presence of uniform flow with $M = 0.37$. Apparently, fictitious eigenfrequencies become an issue in the higher frequency range, and the CHIEF method mitigates the problem.

6. DIRECTIVITIES WITH MEAN FLOW

This section investigates the effect of the flow speed on the directivity of a spatially extended source. The radiator model is a loudspeaker box, shown in Figure 4. The

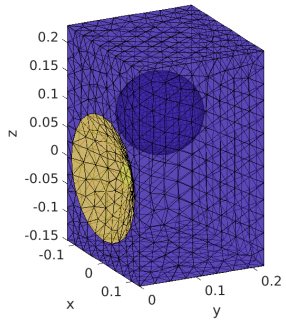

Figure 4. BE mesh of the speaker model. The CHIEF-points are the nodes of the internal sphere.

mesh consists of 1 472 triangular elements, each having three degrees of freedom, located in the three Gaussian quadrature base points, resulting in a piecewise linear discontinuous interpolation of both the sound pressure and normal particle velocity. The loudspeaker is excited by unit surface velocity along the membrane, pointing into the main direction of radiation ($-y$ in the figure). This results in different normal velocities over the membrane. The CHIEF method is applied using control points around the surface of an internal sphere, also visible in the figure. The directivity is evaluated along a horizontal circle of radius $R = 1\,\mathrm{m}$ around the membrane centre.

The obtained directivities are displayed in Figure 5 for flow velocities parallel with the x axis and ranging from $M = 0$ to $M = 0.7$. As expected, the flow results in a shift of the main lobe and the zeros in the flow direction. The directivity loses its symmetry for the $M > 0$ case. The side lobes are attenuated in the upstream side, while amplified on the downstream side of the speaker.

7. MOVING DIRECTED SOURCE

As a demonstrative example, this section presents the simulation of the sound pressure time history observed at a fixed listener position during the passby of the loudspeaker modelled in the previous section. The speaker travels at a velocity $v = 50\,\mathrm{m\,s^{-1}}$, at a distance $D = 5\,\mathrm{m}$ from the x axis, as shown in Figure 6, and emits a harmonic signal at a source frequency $f_0 = 500\,\mathrm{Hz}$. The listener is located in the origin of the coordinate system, and the speaker reaches the $x = 0$ position at $t = 0$. The loudspeaker is rotated horizontally with a $45°$ angle towards the direction of the passby.

The passby is simulated in the time range $-T/2 < t < T/2$, where $T = 3\,\mathrm{s}$, with a sampling frequency $f_s = 5 \times 5\,\mathrm{kHz}$. Here $5\,\mathrm{kHz}$ is the „source sampling frequency" that is sufficient to accurately sample the source signal, and the $5\times$ oversampling is needed to reduce the attenuating effect of the convolution quadrature method. The above parameters result in $75\,000$ sampling points in time domain, or $75\,000/2$ complex sampling points in the complex frequency (s-) domain. However, as demonstrated in Figure 2(b), the transfer needs to be evaluated along a closed trajectory in the s-domain, and a significant part of this trajectory corresponds to s values with large real parts. Due to the kernel function's $\mathrm{e}^{-s\tau}$-like behaviour, the kernel becomes highly damped in this regime. In the present modelling case, the kernel was truncated to those frequencies where

$$\left|\mathrm{e}^{-sD/c}\right| > 10^{-q}, \qquad q = 2. \tag{26}$$

The above rule remarkably reduced the number of actual frequencies, i.e. BEM solutions, from 37 500 to 5695, while not affecting the accuracy of the solution significantly. This has been validated by computing the sound radiation of a moving monopole source using the same parameters.

The transfer function in the moving frame of reference was evaluated in 3000 field points located along the x axis, with a spacing of $\Delta x = 5\,\mathrm{cm}$. As the convolution quadrature method evaluates the kernel in the frequency domain with positive real values of s, the problem of fictitious eigenfrequencies is mitigated by the introduced damping. As a consequence, the CHIEF method does not need to be applied in this case.

The time domain simulation results in the moving frame of reference are shown in Figure 7. Diagram (a) displays the magnitude of the space-time representation. The causal excitation is clearly visible in the form of a conical response. The spatial asymmetry of the magnitude distribution is a combined effect of inclination of the source and the effect of the uniform flow on the directivity.

Figure 7(b) displays the real part of the response, zoomed on a narrow space-time interval around the origin. The bent wave fronts are an effect of the finite source-receiver distance $D = 5\,\mathrm{m}$.

Transforming back to the frame of reference fixed to the receiver, the space-time representation is interpolated along a straight diagonal line, displayed in Figure 7(a). Clearly, this diagonal interpolation results in the proper representation of the Doppler frequency shift. Figure 8

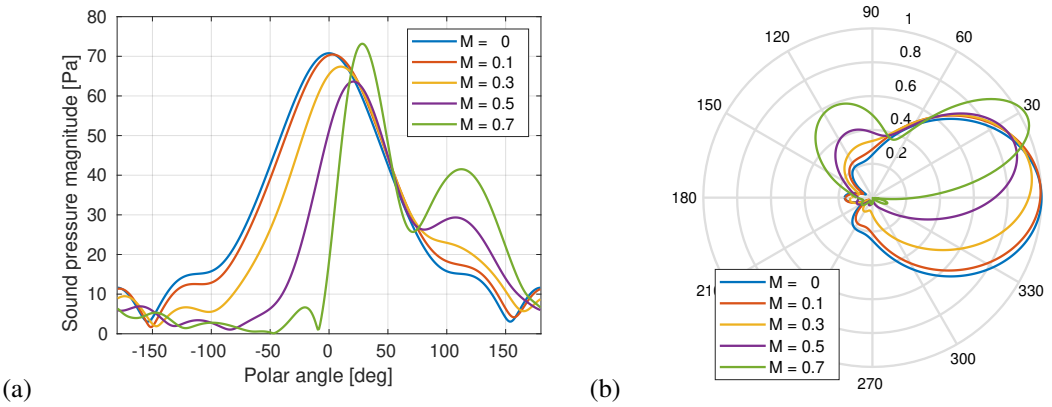

Figure 5. Directivities of the speaker in a horizontal uniform flow with different Mach numbers

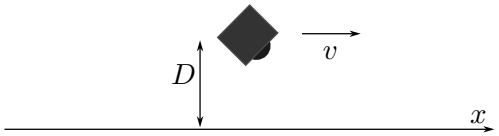

Figure 6. Passby simulation arrangement

displays the response in the fixed frame of reference in the form of a running rms time history and a spectrogram. Both figures show the effect of the causal source in the form of the 0.22 s delay at the beginning of the time histories. The running rms curve highlights the asymmetry of the passby, by comparing the sound pressure level to that radiated by an equivalent moving monopole source. The spectrogram shows the expected Doppler shift.

8. CONCLUSIONS

This paper presented a numerical procedure for computing the sound field of spatially extended moving radiators. The trajectory is restricted to uniform motion resulting in a time-invariant transfer in a frame of reference fixed to the source. Convolution quadratures were applied to transform the system into the complex frequency domain, where independent convected Helmholtz problems need to be solved. The applied frequency domain BEM, extended with the CHIEF method computes the radiated pressure field in a wide frequency range. It was shown how the necessary number kernel evaluations are reduced by exploiting the kernel's high damping behaviour over a significant part of the s-trajectory. After demonstrating the effect of the uniform flow on the directivity of a simple radiator, the time history of a pass-by with a causal excitation signal was computed. It was shown that the presented methodology can address wide band transient pass-by applications with reasonable computation efforts.

9. ACKNOWLEDGMENTS

This work has been supported by the Hungarian National Research, Development and Innovation Office under contract No. K–143436.

10. REFERENCES

[1] P. Zhang and T. Wu, "A hypersingular integral formulation for acoustic radiation in moving flows," *Journal of Sound and Vibration*, vol. 206, no. 3, pp. 309–326, 1997.

[2] X. Liu, H. Wu, and W. Jiang, "A high-order BEM for acoustic problems in a subsonic uniform flow," *Applied Acoustics*, vol. 186, p. 108453, 2022.

[3] M. Kaltenbacher and A. Hüppe, "Advanced finite element formulation for the convective wave equation," in *Proceedings of Euronoise 2018*, (Crete, Greece), pp. 291–295, 2018.

[4] F. Treyssède, G. Gabard, and M. Ben Tahar, "A mixed finite element method for acoustic wave propagation in moving fluids based on an Eulerian–Lagrangian description," *Journal of the Acoustical Society of America*, vol. 113, no. 2, pp. 705–716, 2003.

[5] C. Lubich, "Convolution quadrature and discretized operational calculus. I.," *Numerische Mathematik*, vol. 52, pp. 129–145, 1988.

[6] M. Schanz and H. Antes, "Application of 'operational quadrature methods' in time domain boundary element methods," *Meccanica*, vol. 32, pp. 179–186, 1997.

[7] L. Banjai and S. Sauter, "Rapid solution of the wave equation in unbounded domains," *SIAM Journal of Numerical Analysis*, vol. 47, no. 1, pp. 227–249, 2008.

[8] P. Fiala and P. Rucz, "NiHu: an open source C++ BEM library," *Advances in Engineering Software*, vol. 75, pp. 101–112, 9 2014.

[9] H. A. Schenck, "Improved Integral Formulation for Acoustic Radiation Problems," *The Journal of the Acoustical Society of America*, vol. 44, no. 1, pp. 41–58, 1968.

[10] A. Burton and G. Miller, "The application of integral equation methods to the numerical solution of some exterior boundary-value problems," *Proceedings of the Royal Society of London*, vol. 323, pp. 201–210, 1971.

[11] Y. Saad and H. Schultz, "GMRES: A generalized minimal residual algorithm for solving nonsymmetric linear systems," *SIAM J. Sci. Stat. Comput.*, vol. 7, no. 3, pp. 856–869, 1986.

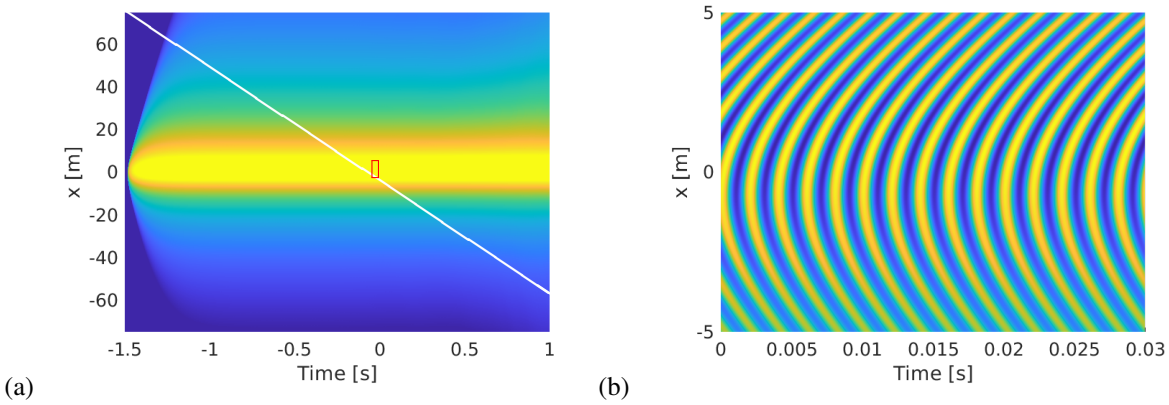

Figure 7. Space-time representation of the radiated sound field in the moving frame of reference. (a) magnitude distribution and (b) real part of the response augmented for a narrow interval (red box)

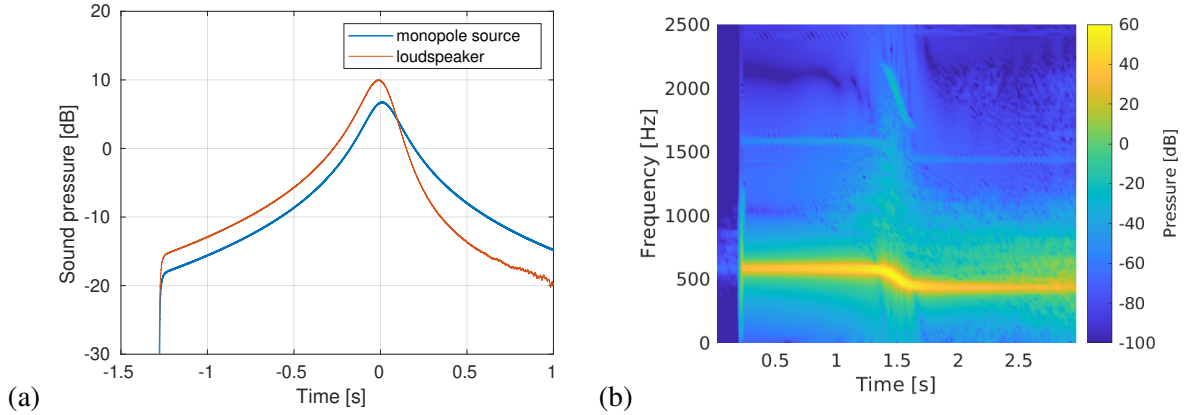

Figure 8. Time history (a) and spectrogram (b) of the passby sound signal in the fixed frame of reference